

# Chemical Differences between K and Na in Alkali Cobaltates

K.-W. Lee and W. E. Pickett

*Department of Physics, University of California, Davis, California 95616*

(Dated: September 7, 2021)

$K_x\text{CoO}_2$  shares many similarities with  $\text{Na}_x\text{CoO}_2$ , as well as some important differences (no hydration-induced superconductivity has been reported). At  $T_{c2} = 20$  K,  $\text{K}_{0.5}\text{CoO}_2$  becomes an insulator with a tiny optical gap as happens in  $\text{Na}_{0.5}\text{CoO}_2$  at 52 K. This similarity, with a known common structure, enables direct comparisons to be made. Using the K-zigzag structure recently reported and the local density approximation, we compare and contrast these cobaltates at  $x=0.5$ . Although the electronic structures are quite similar as expected, substantial differences are observed near the Fermi level. These differences are found to be attributable mostly to the chemical, rather than structural difference: although Na is normally considered to be fully ion, K has somewhat more highly ionic character than does Na in these cobaltates.

PACS numbers: 71.20.Be,71.18.+y,71.27.+a

## I. INTRODUCTION

Takada *et al.* found superconductivity in the layered quasi-two dimensional  $\text{Na}_x\text{CoO}_2$  when intercalating enough water ( $\sim 1.3\text{H}_2\text{O}$ ) to form a separate water layer between  $\text{CoO}_2$  and Na layers.[1] The nonsuperconducting dehydrated  $\text{Na}_x\text{CoO}_2$  system shows a rich phase diagram, which significantly depends on  $x$ . [2] For  $x < 0.5$ , the system shows weakly correlated band-like behavior including Pauli paramagnetism, while the phase  $x > 0.5$  reveals correlated behavior such as large enhancement in linear specific coefficient, Curie-Weiss susceptibility,[3] and magnetic ordering for  $x \geq 0.75$ .

The most peculiar aspect of this system is an insulating phase at  $x = 0.5$ [2] with a tiny gap  $\sim 15$  meV.[4] As the temperature is decreased, antiferromagnetic ordering of some Co spins appears at  $T_{c1} = 88$  K, and at  $T_{c2} = 52$  K there is a gap opening, which reflects the charge-ordering of non-magnetic  $S = 0$  Co1 ions and magnetic  $S = \frac{1}{2}$  Co2 ions.[5, 6] Using neutron diffraction studies, Williams *et al.* inferred the charge difference of  $0.12e$  between Co1 and Co2.[7] This value is much smaller than the  $1e$  value expected from a naive formal charge concept, but is roughly consistent with the theoretically calculated value  $0.2e$  using a correlated band theory LDA+U method.[8, 9] As a result, even though there is small charge difference between the Co ions, the charge-disproportionation is accompanied by local moment formation and the spins are consistent with the formal valences  $\text{Co}^{3+}$  and  $\text{Co}^{4+}$ . [8, 9]

The discovery of an unexpected insulating state in  $\text{Na}_{0.5}\text{CoO}_2$  ( $\text{N}_{0.5}\text{CO}$ ) and hydration-induced superconductivity has stimulated the study of isostructural and isovalent family  $\text{A}_x\text{CoO}_2$  ( $\text{A} = \text{K}, \text{Rb}, \text{Cs}$ ). In spite of a few attempts to produce superconductivity in hydrated  $\text{K}_x\text{CoO}_2$ , the amount of interca-

lated water is 0.8 or less, forming only a monohydrate ( $\text{K}+\text{H}_2\text{O}$ ) layer and no superconductivity has been detected yet.[10, 11]

The  $\text{K}_x\text{CoO}_2$  system has been known for three decades, since Hagenmuller and colleagues reported[12, 13] structure, transport, and magnetic data on phases with  $x=1.0, 0.67$ , and  $0.50$ . Recently, an insulating phase in  $\text{K}_{0.5}\text{CoO}_2$  ( $\text{K}_{0.5}\text{CO}$ ) has been studied in more detail by a few groups;[14, 15] Nakamura *et al.*[16] in the mid-1990s had reported an almost temperature-independent resistivity well above a metallic value. In  $\text{K}_{0.5}\text{CO}$ , using NMR and neutron diffraction studies, Watanabe *et al.* observed similar temperature evolution as in  $\text{N}_{0.5}\text{CO}$ . [15] At  $T_{c1} = 60$  K, a kink in the in-plane susceptibility  $\chi_{ab}$  indicates onset of antiferromagnetic ordering. The resistivity increases sharply at  $T_{c2} = 20$  K, signaling the charge-ordering. At this temperature, there is an additional magnetic rearrangement, indicated by kinks in both  $\chi_{ab}$  and  $\chi_c$ . From  $\mu^+\text{SR}$  experiments Sugiyama *et al.* have obtained similar transition temperatures, 60 and 16 K, in metallic  $\text{K}_{0.49}\text{CO}$ . [17] The former is a magnetic ordering temperature from a paramagnetic state. Based on a mean field treatment of a Hubbard model, they suggested there may be a linear spin density wave (SDW) state between 16 and 60 K, while a commensurate helical SDW state exists below 16 K. Additionally, K or Na ions order (structurally), resulting in formation of a  $2 \times \sqrt{3}$  supercell at  $T_{c0} = 550$  and 470 K for K and Na ions, respectively.[15] The tiny energy gap of similar magnitude with  $\text{N}_{0.5}\text{CO}$  has been observed by Qian *et al.* with ARPES measurements.[14]

Several characteristics of  $\text{N}_x\text{CO}$ , in particular the superconductivity upon hydration and effects of cation ordering, suggest that the behavior in this system is sensitive to details of the electronic structure. The fact that  $\text{K}_{0.5}\text{CO}$  is similar to  $\text{N}_{0.5}\text{CO}$ , yet shows clear differences in behavior, indicates that

TABLE I: Crystal structure comparison between  $K_x\text{CoO}_2$  and  $\text{Na}_x\text{CoO}_2$  at  $x=0.5$ . The orthorhombic structures (space group:  $Pm\bar{m}n$ , No. 59) determined from Na- or K-zigzag ordering are a  $\sqrt{3}a_H \times 2a_H$  superstructure which is based on the hexagonal structure with a lattice constant  $a_H$ . In this structure, the oxygens have three site symmetries, two  $4f$  and one  $8g$ . Here,  $z_O$  is an oxygen height from the Co layers. A main difference in these structures is that  $\text{K}_{0.5}\text{CoO}_2$  has 12 % larger  $c$  lattice constant. The data are from Ref. [7] for  $\text{Na}_{0.5}\text{CoO}_2$  and Ref. [15] for  $\text{K}_{0.5}\text{CoO}_2$ .

parameters	$a_H$ (Å)	$c$ (Å)	$z_O$ (Å)
$\text{Na}_{0.5}\text{CoO}_2$	2.814	11.06	0.971, 0.949, 0.983
$\text{K}_{0.5}\text{CoO}_2$	2.831	12.50	0.965, 0.946, 0.981

a comparison of the electronic structures of these systems is warranted. In this paper, we compare and contrast the two insulating systems  $\text{K}_{0.5}\text{CO}$  and  $\text{N}_{0.5}\text{CO}$ . Here correlation effects and detailed magnetic ordering are neglected, but the observed  $\sqrt{3}a_H \times 2a_H$  supercell including Na/K zigzag ordering is adopted. ( $a_H$  is the hexagonal lattice constant.)

## II. CRYSTAL STRUCTURE AND CALCULATION METHOD

Although some aspects of the structure in the sodium cobaltates are still controversial (especially the alkali metal ordering), all existing information for  $x=0.5$  are based on the basic hexagonal structure. Recently, Watanabe *et al.* observed the orthorhombic  $\sqrt{3}a_H \times 2a_H$  superstructure from a K-zigzag pattern for  $\text{K}_{0.5}\text{CO}$ . [15] For comparison, we have used this orthorhombic structure for both cobaltates. [7, 18] As shown in Table I, in this structure the oxygens have three different site symmetries and slightly different O heights (from the Co layers), leading to distorted  $\text{CoO}_6$  octahedra. The averaged Co–O–Co bond angle is about  $96.5^\circ$  for  $\text{K}_{0.5}\text{CO}$  and  $95.4^\circ$  for  $\text{N}_{0.5}\text{CO}$  (this angle would be  $90^\circ$  for undistorted octahedra). This distortion makes the threefold  $t_{2g}$  manifold split into singlet  $a_g$  and doublet  $e'_g$  bands.

The calculations reported here were carried out within the local density approximation (LDA), using the full-potential local-orbital method (FPLO). [19] The basis sets were chosen as  $(3s3p)4s4p3d$  for Co and K,  $(2s2p)3s3p3d$  for Na, and  $2s2p3d$  for O. (The orbitals in parentheses denote semicore orbitals.) The Brillouin zone was sampled with 98 irreducible  $k$  points.

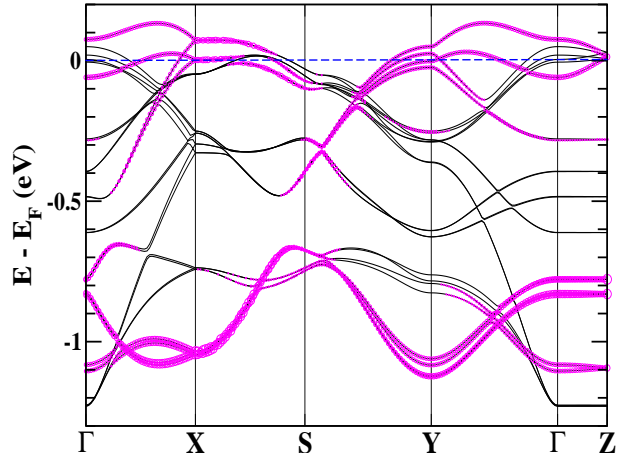


FIG. 1: (Color online) Enlarged band structures of non-magnetic  $\text{K}_{0.5}\text{CoO}_2$  at the  $t_{2g}$  manifold regime. The large  $t_{2g}$ - $e_g$  crystal field splitting of 2.5 eV makes the  $e_g$  manifold (not shown here) unimportant for low energy excitations. The thickened (and colored) lines highlight bands having the strong Co  $a_g$  character. The  $S$  point is a zone boundary along  $\langle 110 \rangle$  direction. The horizontal dashed line indicates the Fermi energy  $E_F$  (set to zero).

## III. RESULTS

### A. Magnetic energy

In  $\text{N}_x\text{CO}$ , the FM state is generically favored energetically within LDA, [3, 20] although this picture is physically correct only for  $0.7 < x < 0.9$ . Our calculations show this tendency is also true for  $\text{K}_x\text{CO}$ . The magnetization energy, defined by the energy difference between nonmagnetic and ferromagnetic states, in  $\text{N}_{0.5}\text{CO}$  is 22 meV/Co, and the energy in  $\text{K}_{0.5}\text{CO}$  slightly increases to 26 meV/Co. The small energy difference can be attributed to the higher magnetic moment on Co in  $\text{K}_{0.5}\text{CO}$ , resulting from longer  $c$  parameter in  $\text{K}_{0.5}\text{CO}$ . (This larger  $c$  lattice constant results in increasing charge of each Co ion by  $0.02e$  in  $\text{K}_{0.5}\text{CO}$ , see below.) From a simple Stoner picture, the small magnetization energy is consistent with small total magnetic moment of  $0.5 \mu_B/\text{Co}$ .

### B. Electronic structure

Now we will focus on the nonmagnetic state to understand the microscopic chemical differences. As observed previously for all  $x$  in  $\text{N}_x\text{CO}$ , [3, 20] the crystal field splitting between the partially occupied  $t_{2g}$  manifold with 1.3 eV width and the unoccupied

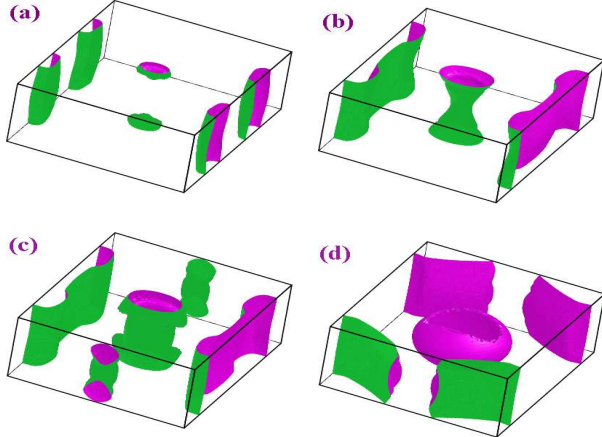


FIG. 2: (Color online) Fermi surfaces of nonmagnetic  $K_{0.5}CoO_2$ , showing strong two-dimensionality. The band structure leads to six Fermi surfaces, but the first and sixth FSs are not shown here. The first FS is similar to (a), except a smaller cap at the Z points. The sixth FS has the same shape as (d), but it has no  $\Gamma$  centered egg. The pink (darker) colored surfaces contain holes, whereas the green (lighter) colored surfaces hold electrons.

$e_g$  manifold with 1 eV width is 2.5 eV. The large splitting makes the  $e_g$  manifold irrelevant for low energy considerations.

The band structure of the  $t_{2g}$  manifold, showing strong two-dimensionality, is given in Fig. 1. (This two-dimensionality is reflected in the Fermi surfaces displayed in Fig. 2.) The  $a_g$  character emphasized by the thickened (or colored) lines is represented by the “fatband” technique in Fig. 1. The  $a_g$  character appears at both the bottom and top of the  $t_{2g}$  manifold, but the character is a little stronger in the bottom. This behavior is also observed in  $Na_{0.5}CoO_2$ .

As expected from the larger  $c$  lattice constant,  $K_{0.5}CoO_2$  has a smaller bandwidth, seen in both the O  $p$  bands (not shown here) and Co  $t_{2g}$  bands. The change in the bandwidth appears clearly at the top valence band in the enlarged band structures near  $E_F$  depicted in the top panel of Fig. 3. The top valence band of  $K_{0.5}CoO_2$  has about 60 meV lower energy at the  $\Gamma$  point and contains less holes, leading to additional  $E_F$ -crossing valence band near the X point and along the  $Y - \Gamma$  line. This crossing produces additional Fermi surfaces of unfolded scroll-like shape along the  $X - S$  line, as displayed in (b) and (c) of Fig. 2. These Fermi surfaces are almost flat near the X point, suggesting enhancement of nesting effects. These nesting effects would lead to SDW, suggested in  $K_{0.49}CoO_2$  by Sugiyama *et al.* Absence of these Fermi surfaces in  $Na_{0.5}CoO_2$  may explain why SDW does not occur in the system.

An important distinction is the stronger two-

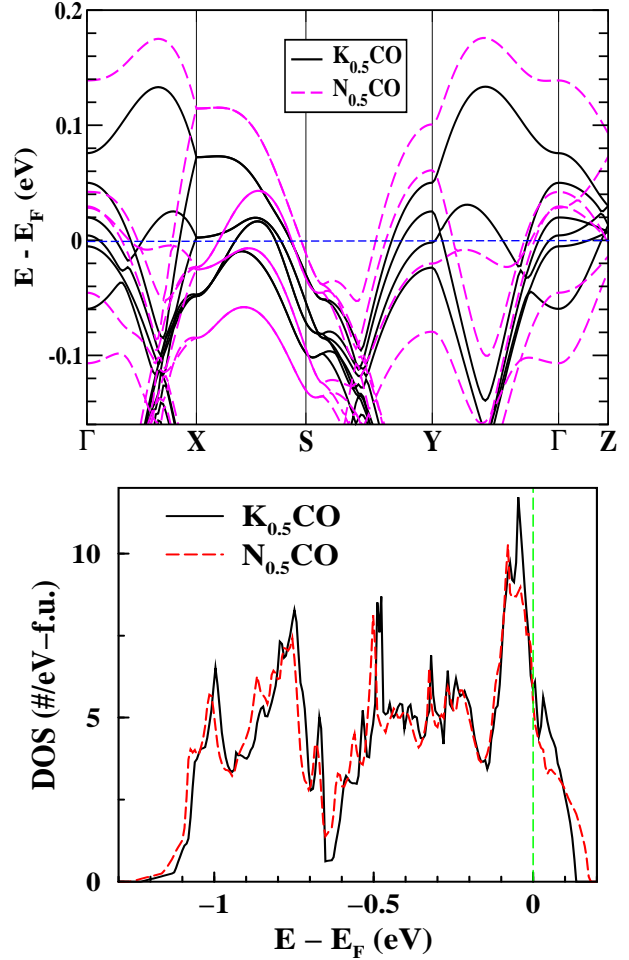


FIG. 3: (Color online) Comparison of electronic structure between nonmagnetic  $K_{0.5}CoO_2$  and  $Na_{0.5}CoO_2$ . Top: Enlarged band structures near  $E_F$ . Differences between the band structures are more noticeable at  $E_F$ , in particular at the X and Y points and along the  $\Gamma$ -Z line. The band structure of  $K_{0.5}CoO_2$  also shows much stronger two-dimensionality. Bottom: Total densities of states per formula unit at the  $t_{2g}$  manifold regime.  $K_{0.5}CoO_2$  has about 10% larger  $N(0)$  than 5.4 states/eV per a formula unit of  $Na_{0.5}CoO_2$  (but invisible in this figure). Here,  $N(0)$  is the density of states at  $E_F$ . The vertical dashed line denotes  $E_F$ .

dimensionality in  $K_{0.5}CoO_2$ . At the X and Y points and along the  $\Gamma$ -Z line, near  $E_F$  there are nearly flat bands and saddle points in  $K_{0.5}CoO_2$ . The bottom panel of Fig. 3 displays a comparison of the DOS of the two cobaltates in the  $t_{2g}$  regime. Strikingly, the Fermi energy (set to zero) of  $K_{0.5}CoO_2$  lies midway between two sharp peaks at  $-45$  and  $35$  meV. In addition, a van Hove singularity appears just above  $E_F$  (at less than 10 meV). These more complicated

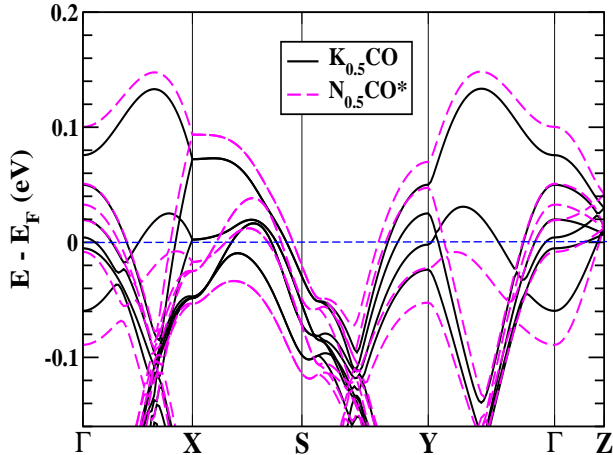


FIG. 4: (Color online) Comparison of band structure between nonmagnetic  $K_{0.5}CoO_2$  and  $Na_{0.5}CoO_2$  near  $E_F$ .  $Na_{0.5}CoO_2$  is assumed to have the same crystal structure as  $K_{0.5}CoO_2$ , in order to investigate pure effects of K substitution.

structures near  $E_F$  lead to 10% higher DOS at  $E_F$ , suggesting an increased tendency toward magnetic instability.

### C. Identifying differences

These differences between two cobaltates can be clarified in two ways. First, we can determine the effects purely due to chemical difference (K vs. Na) as opposed to the size difference leading to structural differences. For this,  $N_{0.5}CO$  is assigned the same structure as in  $K_{0.5}CO$  and denoted  $N_{0.5}CO^*$ . The resulting band structure enlarged near  $E_F$  is compared with that of  $K_{0.5}CO$  in Fig. 4. Even in the identical structure, substantial differences on an important energy scale are evident. The top valence band in  $N_{0.5}CO^*$  is 20 meV higher in energy at the  $\Gamma$  point, although the  $t_{2g}$  bandwidth is about 5% smaller (not shown). Another difference is that the projected K and Na DOS is almost identical (and small, of course) through most of the  $t_{2g}$  bands, except in a  $\sim 0.15$  meV region at and below the Fermi level, where the Na projected DOS (PDOS) is 20-35% larger (more than 50% larger at  $E_F$ ). These distinctions indicate that the differences in electronic structure are mainly due to K substitution itself rather than indirectly through the change in structure.

Second, using the Mullikan charge decomposition, we obtained atom-decomposed charges, which are displayed in Table II. The K ion is very notice-

ably more ionic than the Na ion, consistent with the PDOS difference mentioned just above. The compensating charge is spread over the oxygen ions; the Co charges are essentially the same for  $K_{0.5}CO$  and  $N_{0.5}CO^*$ . This higher ionicity of K seems to be the most discernible difference between these cobaltates.

### D. Comments on hydration

It is still unclear what water does in the system. The only unambiguously aspect is that hydration dramatically increases the  $c$  lattice constant, resulting in more two-dimensionality of the electronic system.[21] However, although the isostructural system  $Na_{1/3}TaS_2 \cdot yH_2O$  shows very similar change in the  $c$  lattice constant when hydrated,[3]  $T_c \approx 4$  K in this system is independent of  $y$ . This difference in behavior established that water has effects in the cobaltates that are not present in the transition metal disulfides and diselenides. In this respect it is interesting that  $(Na_{0.27}K_{0.12})CoO_2 \cdot 0.87H_2O$  shows superconductivity with  $T_c \approx 3$  K and about 7 Å increment in  $c$  lattice constant from  $K_{0.55}CO$ , which is similar in amount to that of hydrated sodium cobaltate.[22]

## IV. SUMMARY

Using a crystal structure recently reported, we have investigated at the LDA level the differences in electronic structure between  $K_{0.5}CoO_2$  and  $N_{0.5}CoO_2$ . Comparison shows a few substantial differences near  $E_F$ ; smaller  $t_{2g}$  bandwidth by 60 meV in  $K_{0.5}CoO_2$ , and additional Fermi surfaces along the  $X - S$  line which are almost flat near the  $X$  point. These differences are due more to chemical differences (higher ionic character of K) rather than to structural difference between the systems.

An angle-resolved photoemission comparison of the three systems  $A_xCoO_2$ ,  $A = Na, K, \text{ and } Rb$ , has appeared,[23] with the differences at equal doping levels being small almost too small to quantify. Unfortunately, samples at precisely  $x=0.5$  were not the focus of that study. Since the superstructure we have studied is confined to  $x=0.5$ , our results cannot be compared with this data. However, the structural disorder of the alkali at  $x \neq 0.5$ , which extends to the  $CoO_2$  substructure, broadens the bands and hides small distinctions.[24] This observation suggests that carrying out spectroscopic studies of both systems in the insulating phase at  $x=0.5$  should be an excellent way to identify and characterize more precisely the effects of the different alkali cations.

TABLE II: Atom-decomposed charges, which are obtained from the Mullikan charge decomposition in the FPLO method, for each atom in  $A_{0.5}CoO_2$  ( $A=Na, K$ ). The absolute numbers do not have a clear meaning, but differences reflect real distinctions in bonding.  $N_{0.5}CO^*$  denotes  $Na_{0.5}CoO_2$  with the same crystal structure as  $K_{0.5}CoO_2$ .

atom site label	A			Co			O			
	$2a$	$2b$	<i>Ave.</i>	$4f$	$4d$	<i>Ave.</i>	$4f$	$4f$	$8g$	<i>Ave.</i>
$K_{0.5}CO$	+0.72	+0.68	+0.70	+1.58	+1.60	+1.59	-0.97	-0.97	-0.97	-0.97
$N_{0.5}CO$	+0.64	+0.63	+0.63	+1.60	+1.62	+1.61	-0.94	-0.97	-0.97	-0.96
$N_{0.5}CO^*$	+0.64	+0.61	+0.63	+1.59	+1.60	+1.59	-0.94	-0.95	-0.96	-0.95

## V. ACKNOWLEDGMENTS

We acknowledge M. D. Johannes and D. J. Singh for illuminating conversations, and D. Qian for clarifying the ARPES data. This work was supported

by DOE grant DE-FG03-01ER45876 and DOE's Computational Materials Science Network. W.E.P. acknowledges the stimulating influence of DOE's Stockpile Stewardship Academic Alliance Program.

- 
- [1] K. Takada, H. Sakurai, E. Takayama-Muromachi, F. Izumi, R. A. Dilanian, and T. Sasaki, *Nature* **422**, 53 (2003).
- [2] M. L. Foo, Y. Wang, S. Watauchi, H. W. Zandbergen, T. He, R. J. Cava, and N. P. Ong, *Phys. Rev. Lett.* **92**, 247001 (2004).
- [3] K.-W. Lee, J. Kuneš, and W. E. Pickett, *Phys. Rev. B* **70**, 045104 (2004).
- [4] N. L. Wang, D. Wu, G. Li, X. H. Chen, C. H. Wang, and X. G. Luo, *Phys. Rev. Lett.* **93**, 147403 (2004); J. Hwang, J. Yang, T. Timusk, and F. C. Chou, *Phys. Rev. B* **72**, 024549 (2005); S. Lupi, M. Ortolani, L. Baldassarre, P. Calvani, D. Prabhakaran, and A. T. Boothroyd, *ibid.* **72**, 024550 (2005).
- [5] M. Yokoi, T. Moyoshi, Y. Kobayashi, M. Soda, Y. Yasui, M. Sato, and K. Kakurai, *J. Phys. Soc. Jpn.* **74**, 3046 (2005).
- [6] G. Gašparovič, R. A. Ott, J.-H. Cho, F. C. Chou, Y. Chu, J. W. Lynn, and Y. S. Lee, *Phys. Rev. Lett.* **96**, 046403 (2006).
- [7] A. J. Williams, J. P. Attfield, M. L. Foo, L. Viciu, and R. J. Cava, *Phys. Rev. B* **73**, 134401 (2006).
- [8] K.-W. Lee, J. Kuneš, P. Novak, and W. E. Pickett, *Phys. Rev. Lett.* **94**, 026403 (2005).
- [9] K.-W. Lee and W. E. Pickett, *Phys. Rev. Lett.* **96**, 096403 (2006).
- [10] G.-C. Fu, C. Dong, M.-X. Li, J. Guo, and L.-H. Yang, *Chin. Phys. Lett.* **22**, 1478 (2005).
- [11] H.-Y. Tang, H.-Y. Lin, M.-J. Wang, M.-Y. Liao, J.-L. Liu, F.-C. Hsu, and M.-K. Wu, *Chem. Mater.* **17**, 2162 (2005).
- [12] C. Delmas, C. Fouassier, and P. Hagenmuller, *J. Solid State Chem.* **13**, 165 (1975).
- [13] C. Fouassier, C. Delman, and P. Hagenmuller, *Mat. Res. Bull.* **19**, 443 (1975).
- [14] D. Qian, L. Wray, D. Hsieh, D. Wu, J. L. Luo, N. L. Wang, A. Kuprin, A. Fedorov, R. J. Cava, L. Viciu, and M. Z. Hasan, *Phys. Rev. Lett.* **96**, 046407 (2006).
- [15] H. Watanabe, Y. Mori, M. Yokoi, T. Moyoshi, M. Soda, Y. Yasui, Y. Kobayashi, M. Sato, N. Igawa, and K. Kakurai, *J. Phys. Soc. Jpn.* **75**, 034716 (2006).
- [16] S. Nakamura, J. Ohtake, N. Yonezawa, and S. Iida, *J. Phys. Soc. Jpn.* **65**, 358 (1996). Compared with the existing data for lattice constants, this sample does not seem to be exact  $x = 0.5$  phase, but  $0.5 < x < 0.55$ . This assumption may be supported by the Curie-Weiss behavior in the sample.
- [17] J. Sugiyama, H. Nozaki, Y. Ikeda, K. Mukai, J. H. Brewer, E. J. Andreica, A. Amato, T. Fujii, and A. Asamitsu, *Phys. Rev. Lett.* **96**, 037206 (2006).
- [18] Q. Huang, M. L. Foo, J. W. Lynn, H. W. Zandbergen, G. Lawes, Y. Wang, B. H. Toby, A. P. Ramirez, N. P. Ong, and R. J. Cava, *J. Phys.: Condens. Matter* **16**, 5803 (2004).
- [19] K. Koepf and H. Eschrig, *Phys. Rev. B* **59**, 1743 (1999).
- [20] D. J. Singh, *Phys. Rev. B* **61**, 13397 (2000).
- [21] C. A. Marianetti, G. Kotliar, and C. Ceder, *Phys. Rev. Lett.* **92**, 196405 (2004); M. D. Johannes and D. J. Singh, *Phys. Rev. B* **70**, 014507 (2004); R. Arita, *ibid.* **71**, 132503 (2005).
- [22] H. Taniguchi, Y. Ebina, K. Takada, and T. Sasaki, *Solid State Ionics* **176**, 2367 (2005).
- [23] T. Arakane, T. Sato, T. Takahashi, H. Ding, T. Fujii, and A. Asamitsu, *J. Phys. Soc. Jpn.* **76**, 054704 (2007).
- [24] D. J. Singh and D. Kasinathan, *Phys. Rev. Lett.* **97**, 016404 (2006).